ISSN 2176-5480

22nd International Congress of Mechanical Engineering (COBEM 2013)
November 3-7, 2013, Ribeirão Preto, SP, Brazil

DAMAGE DETECTION USING ROBUST SINGULAR VALUE DECOMPOSITION METHOD APPLIED TO FRFs AT HIGH FREQUENCY

Horacio V. Duarte
Lázaro Valentim Donadon
Rogério Pinto Ribeiro
Mechanical Engeneering Department at Engeering School of Federal University of Minas Gerais
hvduarte_y@yahoo.com.br

Abstract. *A laminate beam is used to generate vibration data for a healthy and damaged structure. The method employed, Robust Singular Value Decomposition, uses robust statistics to avoid outliers data and the analysis can be done in a set of healthy and damaged data. The algorithm was used to find the minimal distance between a measurement set and its best subset to avoid great measurement errors. The measurement data are frequency response functions, FRFs, forming the columns of the database matrix. The main assumption is that high frequency FRFs are more sensitive to small damages. Remarks are made on efficiency and sensitivity of the detection algorithm for different damage levels and measurement techniques.*

Keywords: *Singular value decomposition, Structural health monitoring, laminated composite, damage detection.*

1. INTRODUCTION

In order to reduce conservative project and equipment maintenance costs, and due to an increasing use of new materials the health structural monitoring has gained increasing attention of the scientific community. The composite structures have a damage mechanism different from those of metals that they are replacing and failure detection need to be improved.

Changes in dynamic response of the structure are linked to a change in stiffness, mass or damping of the structure and this is the basic idea of structural health monitoring, Shane and Jha (2011). Many techniques proposed to detect damage are based in changes in modal parameters, a comprehensive review on modal parameters-based damage identification can be found in Fan (Fan and Qiao, 2011).

Another method is the ultrasonic guided waves, in particular Lamb waves, that is aimed at plate-like structures, Konstantinidis G. (2006) . Its ability to detect defects have been demonstrated by published results. The measurements are made using high frequency PZT sensors. Being thin and light they can be bonded or embedded on the structure. There are another methods in research, sensors and monitoring strategies, that will not mentioned here.

The use of modal analysis on structural health monitoring is a natural consequence of its use on dynamic behavior of structure analysis. However, a major concern is that its validity is limited to linear structures, Kerschen *et al.* (2005). Vanlanduit, (Vanlanduit *et al.*, 2005) said that methods based on modal parameters are sensitive to changes in environment, operational conditions and structural uncertainties. The proper orthogonal decomposition (POD) method has been proposed aiming to remove the influence of these external factors Vanlanduit *et al.* (2005) and Shane and Jha (2011).

The proper orthogonal decomposition (POD) is a powerful multi-variate statistical method for data analysis aimed at obtaining low-order approximate descriptions of a high-dimensional process, C. Wu (2003). The POD is an orthogonal transformation that decorrelates the signal components and maximizes variance. By this way the POD method reduce a large number of interdependent variables to a much smaller number of uncorrelated variables while retaining as much as possible of the variation in the original variables (Kerschen *et al.*, 2005) The discrete implementation of the proper orthogonal decomposition is the popular singular value decomposition, G. Kerschen (2002)C. Wu (2003).

There are different implementations of the proper orthogonal decomposition method to structural health monitoring. Vanlanduit, Vanlanduit *et al.* (2005), proposed the robust singular value decomposition method (RSVD) that uses the frequency response functions (FRFs) of displacement, force, acceleration or other output as a basic data for the method.

As the RSVD presented good results employing FRF (frequency response functions) this procedure was used to analyse the FRFs of an Aluminum 2024-T4 laminated beam. The measurements were made by using high frequency PZT sensors from healthy beam and from this beam with two different delamination levels.

This work is closely related to implementation of the robust singular value decomposition method (RSVD) as published by Vanlanduit, Vanlanduit *et al.* (2005), which could find fault signals on a set with healthy and damaged data. The main objective is the experimental sensitivity verification of the method with PZT sensors that could be embedded in structure a procedure of the health structural monitoring, Konstantinidis G. (2006). The bonded PZT sensors allowed good repeatability of measurements, essential to method, and measurements in a high frequency range. The main assumption is that smallest faults can be found by changes in highest mode frequencies and the Vanlanduit method was developed to first natural frequencies.

ISSN 2176-5480

2. Damage Detection Algorithm

The classical Least-Squares SVD-based damage detection can be outlined as follow. The database is obtained from frequency response function, FRF, a $M \times N$ matrix $H = [H_1, H_2, ...H_N]$ at N specified conditions, each matrix H_n has FRF data from each P specified positions. $N = N_u + N_d$ where N_u is the undamaged experimental FRFs from healthy structure and N_d is from damaged ones. The damaged database $N_D = \sum N_d$ must be equal or greater than $N_U = \sum N_u$. The sequence steps of the damage detection algorithm are presented below.

1- Computing the SVD of the $M \times N$ matrix $H = USV^H$;
2- Putting all singular values $s_{k+1}, ..s_N$, from $S = diag(s_1, s_2, .., s_N)$, bellow the noise level equals zero, $S1 = diag(s_1, s_2, .., s_k, 0, 0, .., 0)$;
3- Using singular vectors U and V from original matrix synthesize matrix $H1$ of rank k $H1 = US1V^H$;
4- Computing residual matrix $E1$, $E1 = H - H1$;
5- Computing the variance s of the residuals:

$$s = \frac{1}{MN - 1} \sum_{i=1}^{M} \sum_{j=1}^{N} (H_{i,j} - H1_{i,j})^2 \qquad (1)$$

6- Computing the variance of each measurement j (each column j):

$$s_j = \frac{1}{M - 1} \sum_{i=1}^{M} (H_{i,j} - H1_{i,j})^2 \qquad (2)$$

7- Estimating the relative distance d_j^{SVD} of each measurement j to subspace computed by SVD:

$$d_j^{SVD} = \frac{s_j}{s} \qquad (3)$$

As the relative distance d_j^{SVD} is defined as a variance ratio it obeys a χ^2 distribution. For a χ^2 distribution with a confidence level of $(100 - \alpha) = 95\%$ and for $(N_n - 1)$ degrees of freedom or equal to 30 $(N_n - 1) > 30$, (Vanlanduit *et al.*, 2005), a threshold T can be defined as

$$T = \sqrt{\frac{\chi^2_{(100-\alpha)_{(N_n-1)}}}{2}} \qquad (4)$$

2.1 The Robust SVD

The problem with the LS-SVD based damage detection is that it is very sensitive to outliers in measurements Vanlanduit, Vanlanduit *et al.* (2005). To avoid this the robust method was proposed, and it did not compute the whole database H, the SVD is computed only over $N/2$ observations, the original matrix is re-synthesized and the distances and the error are computed. The solution is the small cost function from all possible combinations of the database. The steps of the RSVD routine are:

1- Construct a matrix H_R from matrix H with $L = N/2$ combination columns from N columns of the original matrix.

a- compute the SVD of the matrix $H_R = U_R S_R V_R^H$;

b- compute the extended right singular vector $V_E = U_R^H S_R^{-1} H$;

c- computing re-synthesized matrix H_S using $H_S = U_R S_E V_E^H$, $S_E(i,i) = S_R(i,i)$ $i = 1, 2, ..., L$ and $S_E(i,i) = 0$ if $i > L$;

d- Computing the residuals $E_S = H - H_S$;

e- Computing the variance s of the residuals using the median absolute deviation MAD, as in [4], $s = MAD(E_S)$, where:

$$MAD(E_S) = 1.4826 * median(|E_S - median(E_S)|) \qquad (5)$$

f- Computing the variance of each measurement j (each column j):

$$s_j = \frac{1}{M - 1} \sum_{i=1}^{L} (H_{i,j} - H_{S(i,j)})^2 \qquad (6)$$

ISSN 2176-5480

g- Estimating the relative distance d_j^{SVD} of each measurement j to subspace computed by SVD:

$$d_j^{SVD} = \frac{s_j}{s} \tag{7}$$

h- compute the cost function $\kappa = \sum_j^L |d_j|^2$;

2- The smallest cost function κ is taken as the RSVD solution, $H_B = H_S$. The variance s and d_j^{SVD} are computed following the procedures from **d** to **g** in the previous steps. As the relative distance d_j^{SVD} is defined as a variance ratio it obeys a χ^2 distribution. For a χ^2 distribution, the threshold T is the same as defined on Eq. 4 and there was employed the same confidence interval.

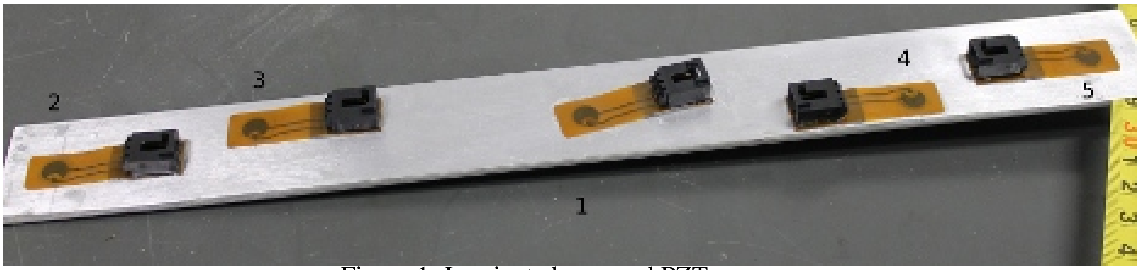

Figure 1. Laminate beam and PZT sensors.

3. Material and testing procedure

The experimental procedure was done using dynamic response of a free-free laminate beam made by 4 Aluminum 2024-T4 0.46 mm thick (0.018 inch) plates and epoxy resin. The laminate beam has 300 mm length, 32.5 mm wide with a total thickness of 2.0 mm. The measurement database was obtained from FRF response at 4 measurement points, 2, 3, 4 and 5, Fig. (10). Points 2 and 5 are on longitudinal axis and are symmetric about center, point 1, and point 3 and 4 are lateral and anti-symmetric. The measurement points 4 and 5 are nearest to failure area, Fig. (2), and both were also used to excite the system as they provide high level vibration as active sensor than others. The point 1 was used as a reference

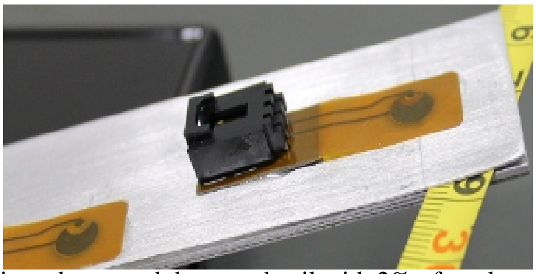
Figure 2. Laminate beam and damage detail with 2% of total area delaminated.

point to obtain the FRFs as the measurement signal level were different from sensors to sensor. Using the passive signal of point 1 as reference for FRF do not change the results but reduce the dispersion in signal level. A measurement run were made for the healthy laminate beam, another database were taken from this beam with a delaminate area of 195 mm^2, 2% of the total area, and another measurement run for the beam with a delaminated area of 504 mm^2, 5% of the total area.

The experimental data acquisition set was the PHOTON II Dynamic Signal Analyzer and all type of excitation signal employed was also generated by this equipment. The white noise, uniform random, sweep sine signals from the PHOTON II were amplified and sent to PZT 4 or 5, Fig. (10). All FRFs have units Volts/Volts (response/excitation) in a frequency range from 0 to 37500 Hz. The PZTs sensors are from Acellent Technologies.

4. Results and data analysis

Two experimental sets were made one of them the PZT 2, in longitudinal line, and lateral PZTs 3 and 4 are passive or measurement sensors, the PZT 5 was active or excitation point receiving the signal from the amplifier, this configuration will be named configuration A, Fig. (3). The configuration B was that where PZTs 2,3 and 5 were measurement sensors and the lateral PZT, at point 4, was the the active sensor responsible for system excitation receiving the amplified signal , Fig. (3).

On Figure (4) there are coherence for *sweep sine* excitation signal, at bottom the FRFs from which the coherence was obtained. As PZT sensors is for high frequency, the coherence does not exhibit good values for low frequency, as

ISSN 2176-5480

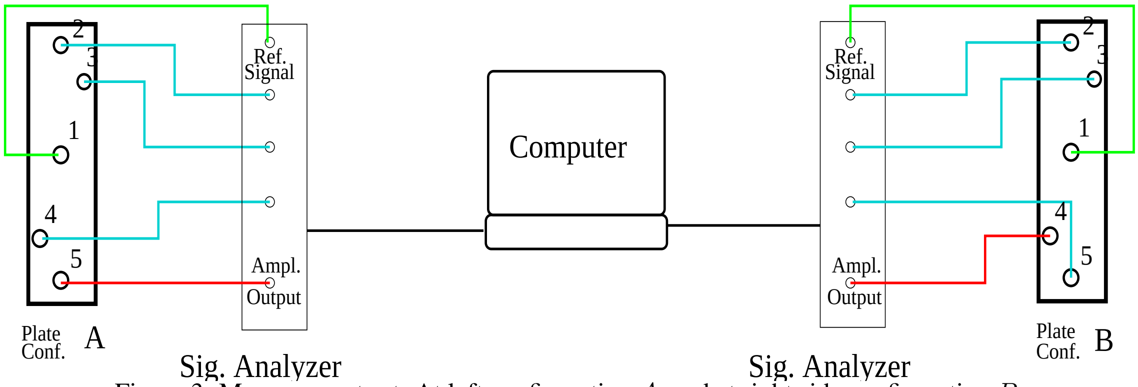

Figure 3. Measurement set. At left configuration A, and at right side configuration B.

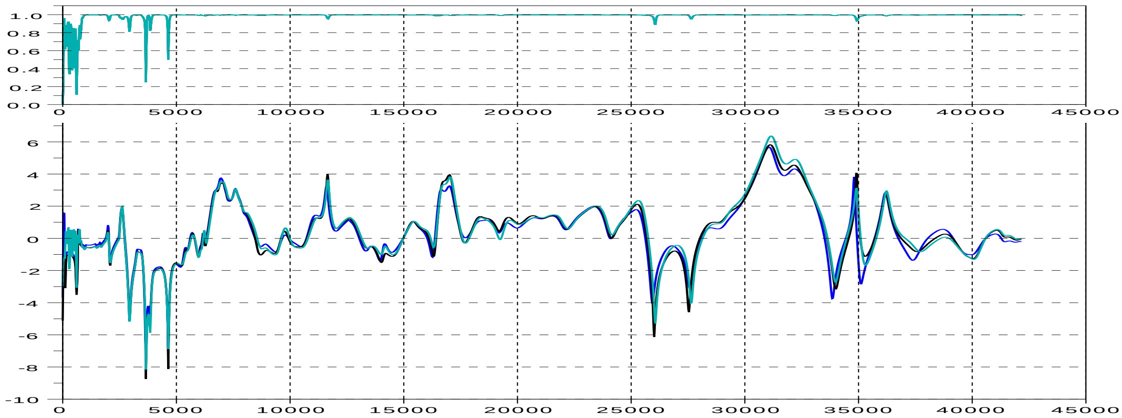

Figure 4. *Sweep sine* coehence, at top, and the FRFs for 2% damaged plate.

expected, and the FRFs had low amplitude too. The *sweep sine* excitation was set up to 0.91 sec/sweep and frequency range was from 1.0 kHz to 37.5 kHz and this set up behavior can be observed on graphic. The majority of results presented in this work made use of *sweep sine* excitation for frequencies above 5000 Hz.

The results presented on Fig. (4) are from a 2% damaged beam with excitation on lateral PZT, point 4, configuration B, and response measured on PZT 5. This point presented the worst behavior related to coherence as it had a low level response signal. The coherence signal was used here as criteria to discard some experimental results.

4.1 Results for 2% damaged structure

The FRFs, in logarithm scale, for the healthy and 2% damaged structure are on Fig. (5) for excitation at PZT 5. On Fig. (5) there are only FRFs for measurement PZTs at positions 2 and 3, black lines for healthy and red lines for damaged structure. For the healthy structure, before being damaged, the FRFs for point 3 was plotted with a thicker line and has a low signal level than the FRF for point 2 as stated before. For damaged structure the response signal for points 2 and 3 were close and the FRF lines are almost not differentiable as the response signals level of point 3 raised.

On Fig. (5) there are strong changes on the FRF shape for equivalent measurement points for all frequency range. There were no natural modes with the same or closed values for frequency or amplitude. As there are few measurement points it is not possible a modal analysis to identify each frequency mode and its change but there is no doubt that failure is responsible for changes.

On Fig. (6) there are only FRFs for measurement points at positions 2 and 3, black lines for healthy, point 3 strong lines, and red lines for damaged structure as the response signal for points 2 and 3 had close response.

A strong change in FRFs shapes can be observed in this configuration as observed in the previous one. But there are what could be seemed as similar measurement frequency behavior between healthy and damaged than one can observe for configuration A. As stated before, there are no confidence to make this analysis as there are no modal analysis to associate frequency and mode. The signal level of the passive PZT 3 had raised to a level close of the PZT2 as in previous case.

The same observations can be made about the FRFs for the 5% damaged structure as stated for the 2% damaged.

ISSN 2176-5480

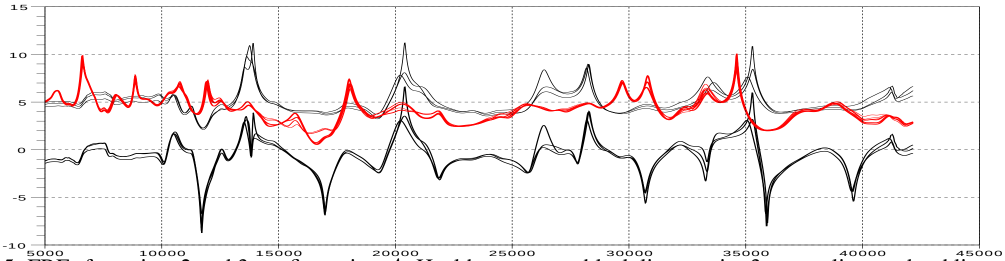

Figure 5. FRFs for points 2 and 3 configuration A. Healthy structure black lines, point 3 strong line, and red lines for 2% damaged one.

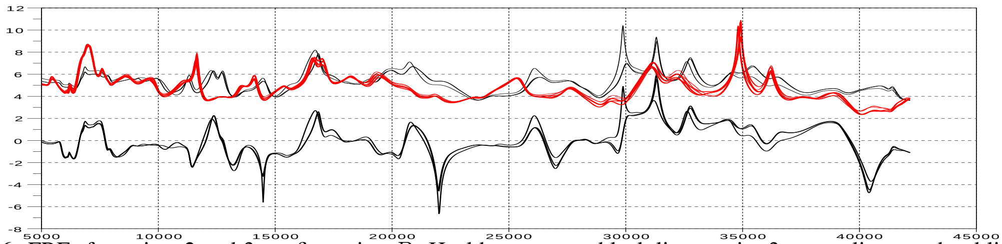

Figure 6. FRFs for points 2 and 3 configuration B. Healthy structure black lines, point 3 strong lines, and red lines for 2% damaged one.

There were no natural modes with the same or closed values for frequency or amplitude and signal level on passive PZT 3 had the same level as the PZT 2 and the response curve of this sensors are close in both configurations and in both measurements.

On Fig. (7) are plotted the FRFs for 2 and 5% damaged structures. This graphic was made only for configuration B as the results were more close. The FRFs from measurement PZTs 2 and 3 for damaged structures are more similar than the healthy and 2% delaminated composite beam. The main difference in FRFs are in two frequency modes inside the range from 29 kHz to 33 kHz. The frequency modes are like and for 5% damaged structure, red lines, they show a highest amplitude at lowest frequency than the 2% damaged, black lines. Indeed the frequency modes for the 5% damaged presented low frequencies than the 2% damaged structure for the whole frequency band.

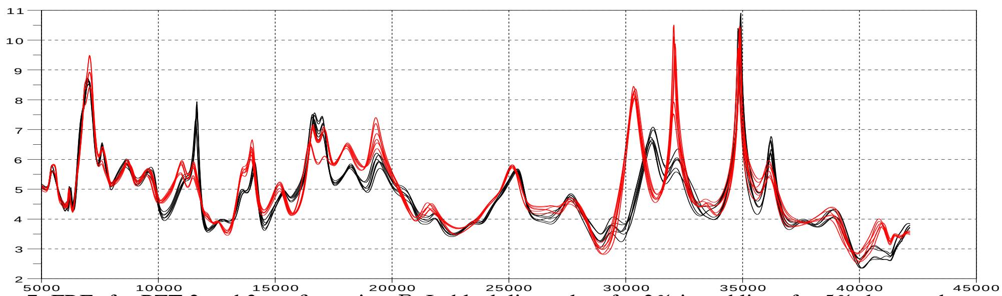

Figure 7. FRFs for PZT 2 and 3 configuration B. In black lines plots for 2% in red lines for 5% damaged structure.

The deviation of the 5% and 2% delaminated structure from the healthy measurement were more significant than expected. There is no conclusive explanation for this behavior, but being the failure near to a stressed lamina it can lead to a expressive stiffness reduction. Another explanation is that the free lamina tip of the beam can hit the surface creating a nonlinear effect. Probably both effects can be present.

4.2 Numerical results

The numerical results were obtained following RSVD routine , the only change was related to use of genetic algorithm for minimizing the cost function. In this work was employed a algorithm of Scilab software.

The RSVD routine had not presented good results for analysis of failure employing healthy and damaged data. An explanation is that the natural frequencies in the FRFs for healthy and damaged structure are not similar and the FRFs are not recognized as being a change in the same pattern. To test this hypothesis the RSVD algorithm was used with 2% and

ISSN 2176-5480

5% damaged structure data in configuration B as they showed nearest FRFs as it could be saw on Fig. (7). The data for 2% damaged structure were considered as reference.

Using the RSVD procedure 9 FRF measurements were selected from 36 measurements of 2% damaged data. The 9 FRFs combinations of all possible 9 combinations of the 36 FRFs from database that resulted in best cost function κ were taken as representative of this reference population. To do this there were used a genetic algorithm for a population of 1200 individuals, 1300 couples, with crossover probability of 90%, mutation probability of 50%.

Before applying the RSVD method, the best data from the 2% damaged structure was used as reference in a matrix formed with these data and all data of 5% damaged. Those selected data from the reference (2% damaged) was taken as reference matrix H_R, the first step of the RSVD routine, and the distances from the re-synthesized matrix H_S to matrix H were computed and those results are on Fig. (8). The H matrix is a matrix with 18 FRFs, 9 of them were the selected from reference and 9 measurements were all measurements of the 5% damaged structure in configuration B, without any pre-selection.

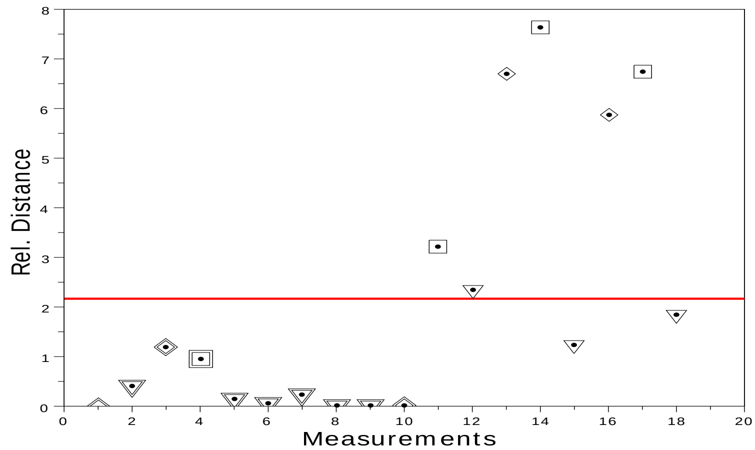

Figure 8. Threshold in red line and relative distances using 9 best experiments from 2% data set as reference and 5% data of delaminated beam.

On Fig. (8), the results showed the relative distance for the 2% damaged reference data, the first 9 points with double concentric symbols, and 5% damaged the last points plotted with single symbol. The point 2, position showed in Fig. (10), were plotted using a symbol structure showed almost all points above computed threshold T for the sample size of 18 FRFs. The only two points in this database that did not indicate failure are FRFs corresponding to measurement at PZT 5.

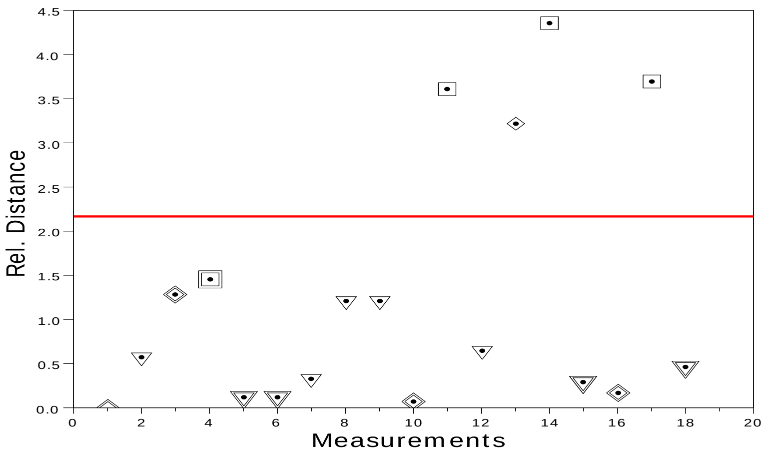

Figure 9. Threshold in red line and relative distances points using RSVD routine. First 9 points from 2% data and last 9 points belonging to 5% damaged beam.

Applying RSVD method as described previously to system with 9 selected data from the reference and all 9 FRFs

ISSN 2176-5480

data for 5% damaged structure the results were plotted on Fig. (9). The symbols are the same employed in previous figure and double symbols correspond to combination that generates the subspace with best cost function. There were 4 measurements which distance is greater than the threshold value. These points with damage indication were also obeserved in the previous analysis, Fig. (8). The majority of measurement points which presented small distances d_j^{SVD} were taken at position 5 ('$\bigtriangledown$').

It is an unexpected result as the PZT 5 is nearest to the fault place and it should present a relative distance greater than threshold. There were 6 measurements taken at point 5 from 9 selected points from 2% reference data. Probably the measurements at point 5 were not acknowledged as change in the pattern but a new pattern. Another explanation is that the FRFs from reference to 5% damage did no change so much or its change level were not significant.

5. Closing remarks

For those presented data the algorithm can be considered effective to indicate only that there is a failure in the structure. But this procedure did not indicate a correct position of the failure. It is very sensitive to small deviations from the pattern but it does not seem to be able to identify pattern changes as it is expected from a significant fault.

The algorithm has been developed for identifying structural faults using the first modes whose frequencies are generally little affected by small failures. Of course those results must be considered as preliminary data, but the sensitivity to small changes on FRF data should be considered a positive aspect of the method as the high frequency modes has been showed more sensitive to failures. A drawback is that using only few measurement points it is not possible to do a modal analysis identifying changes in shape modes and or if there is a change in position between different modes.

More experiments are also needed to verify if different signal level could interfere in the results and to analyse the change in signal level at PZT 3 observed in tests with the damaged structure. To generalise results other length to width ratio must be investigated and also behavior changes by moving delamination to inner layers.

6. References

7. TEXT FORMAT

The manuscripts should be written in English, typed in A4 size pages, using font Times New Roman, size 10, except for the title, authors affiliation, abstract and keywords, for which particular formatting instructions are indicated above. Single space between lines is to be used throughout the text.

The text block that contains the title, the authors' names and affiliation, the abstract and the keywords must be indented 0.1 cm from the left margin and marked by a leftmost black line border of width 2 1/4 pt.

The first page must have a top margin of 3 cm and all the other margins (left, right and bottom) must have 2 cm. All the other pages must be set with all margins equal to 2 cm.

PAGES **SHOULD NOT** BE NUMBERED

The body of the text must be justified. The first line of each paragraph must be indented by 0.5 cm. Sufficient information must be provided directly in the text, or by reference to widely available published work. Footnotes should be avoided.

All the symbols and notation must be defined in the text. Physical quantities must be expressed in the SI (metric) units. Mathematical symbols appearing in the text must be typed in italic style.

Bibliographic references should be cited in the text by giving the last name of the author(s) and the year of publication, according to the following examples: "Recent work (de Oliveira and Melo, 2013)" or "Recently, McConnell and Varoto (2008)". In the case of three or more authors, the form "Rodriguez *et al.* (2006)" should be used. Two or more references having the same authors and publication year must be distinguished by appending "a", "b", etc., to the year of publication. For example: "Recent work (Trindade and Benjeddou, 2011a)".

Acceptable references include journal articles (Trindade and Benjeddou, 2011a), numbered papers, dissertations, theses (Lee, 2003), published conference proceedings (de Oliveira and Melo, 2013; Rodriguez *et al.*, 2006; Trindade and Benjeddou, 2011b), preprints from conferences, books (McConnell and Varoto, 2008), submitted articles (if the journal is identified) and private communications (Clark, 1986). Internet sites can also be cited as references (ABCM, 2004; MLA, 2004).

References should be listed at the end of the paper according to instructions provided in Section 4.

ISSN 2176-5480

7.1 Section titles and subtitles

The section titles and subtitles must be aligned at left, typed with Times New Roman, size 10, bold style font. They must be numbered using Arabic numerals separated by points. No more than 3 sublevels should be used. One single line must be included above and bellow each section title/subtitle.

7.2 Mathematical equations

The mathematical equations must be indented by 0.5 cm from the left margin. They must be typed using Times New Roman, italic, size 10 pt. font. Arabic numerals must be used as equation numbers, enclosed between parentheses, right-aligned, as shown in the examples below. Equations should be referred to either as "Eq. (8)" in the middle of a phrase or as "Equation (8)" in the beginning of a sentence. Matrix and vector quantities can be indicated either by brackets and braces, as in Eq. (8), or in bold style, as in Eq. (9). Symbols used in the equations must be defined immediately before or after their first appearance.

One single line must be included above and bellow each equation.

$$[M]\{\ddot{x}\} + [C]\{\dot{x}(t)\} + [K]\{x(t)\} = f(t) \tag{8}$$

$$\mathbf{M}\ddot{\mathbf{x}}(t) + \mathbf{C}\dot{\mathbf{x}}(t) + \mathbf{K}\mathbf{x}(t) = \mathbf{f}(t) \tag{9}$$

7.3 Figures and tables

Figures and tables should be placed in the text as close as possible to the point they are first mentioned and must be numbered consecutively in arabic numerals. Figures must be referred to either as "Fig. 10" in the middle of a phrase or as "Figure 10" in the beginning of a sentence. The figures themselves as well as their captions must be centered in the breadth-wise direction. The captions of the figures should not be longer than 3 lines.

The legend for the data symbols as well as the labels for each curve should be included into the figure. Lettering should be large enough for ease reading. All units must be expressed in the S.I. (metric) system.

One blank line must be left before and after each figure.

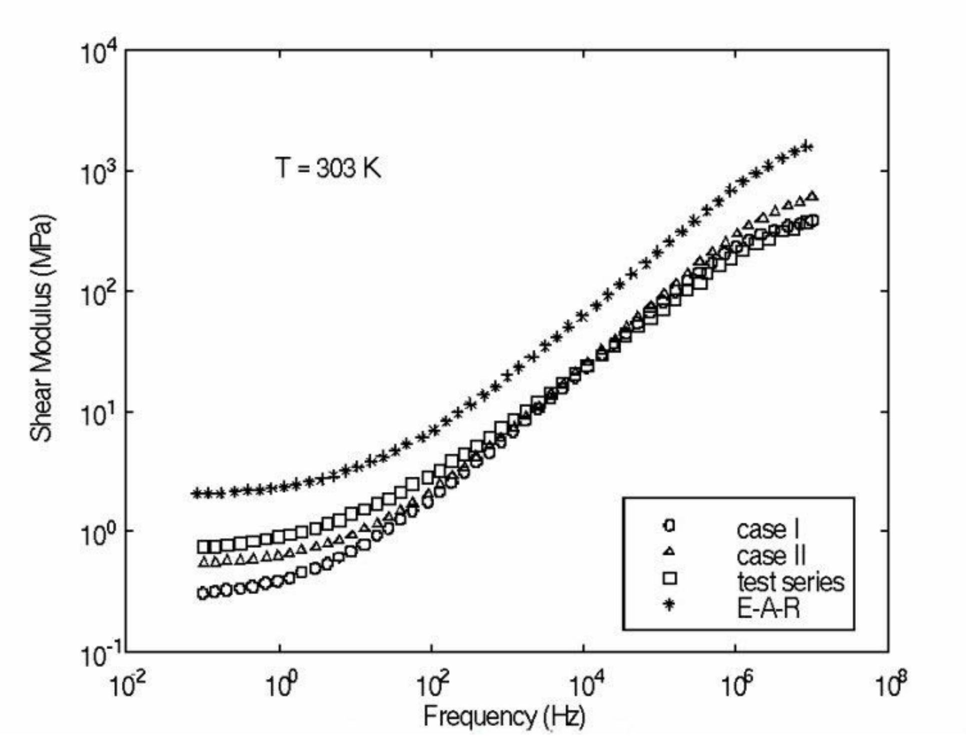

Figure 10. Diagram of shear modulus versus frequency at 303 K

Color figures and high quality photographs can be included in the paper. To reduce the file size and preserve the graphic resolution, figures must be saved into GIF (figures with less than 16 colors) or JPEG (for higher color density) files before being inserted in the manuscript.

Tables must be referred to either as "Tab. 1" in the middle of a phrase or as "Table 1" in the beginning of a sentence. The tables themselves as well as their titles must be centered in the breadth-wise direction. The titles of the tables should

ISSN 2176-5480

not be longer than 3 lines. The font style and size used in the tables must be similar (both in size and style) to those used in the text body. Units must be expressed in the S.I. (metric) system. Explanations, if any, should be given at the foot of the tables, not within the tables themselves.

One blank line must be left before and after each table.

The style of table borders is left free. An example is given in Tab. 1.

Table 1. Experimental results for flexural properties of CFRC-4HS and CFRC-TWILL composites.
Span/depth ratio = 35:1. Average results of 7 specimens.

Composite Properties	CFRC-TWILL	CFRC-4HS
Flexural Strength (MPa)$^{(1)}$	209$\pm$ 10	180 $\pm$ 15
Flexural Modulus (GPa)$^{(1)}$	57.0 $\pm$ 2.8	18.0 $\pm$ 1.3
Mid-span deflection at the failure stress (mm)	2.15 $\pm$ 1.90	6.40 $\pm$ 0.25

$^{(1)}$ measured at 25^{o}C

8. ACKNOWLEDGEMENTS

This optional section must be placed before the list of references.

9. REFERENCES

The list of references must be introduced as a new section, located at the end of the paper. The first line of each reference must be aligned at left. All the other lines must be indented by 0.5 cm from the left margin. All references included in the reference list must have been mentioned in the text.

References must be listed in alphabetical order, according to the last name of the first author. See the following examples:

ABCM, 2004. "Journal of the Brazilian Society of Engineering and Mechanical Sciences". 1 Feb. 2007 <http://www.abcm.org.br/journal/index.shtml>.

Clark, J.A., 1986. *Private Communication*. University of Michigan, Ann Harbor.

de Oliveira, L.P.R. and Melo, F.X., 2013. "Tpa as a tool for the desing of active noise control". In *Proceedings of the International Symposium on Dynamic Problems of Mechanics - DINAME2013*. Buzios, Brazil.

Fan, W. and Qiao, P., 2011. "Vibration-based damage identification methods: A review and comparative study". *Structural Health Monitoring*, Vol. 10(1), pp. 83–111.

Kerschen, G. and Golinval, J.C., 2002. "Physical interpretation of the proper orthogonal modes using the singular value decomposition". *Journal of Sound and Vibration*, Vol. 249(5), pp. 849–865.

Kerschen, G., Golival, J., Vakakis, A.F. and Bergman, L.A., 2005. "The method of proper orthogonal decomposition for dynamical characterization and order reduction of mechanical systems: an overview". *Nonlinear Dynamics*, Vol. 41, pp. 147–169.

Konstantinidis, G., Drinkwater, B.W. and Wilcox, P.D., 2006. "The temperature stability of guided wave structural health monotoring system". *Smart Materials and Structures*, Vol. 15, pp. 967–976.

Lee, Y.B., 2003. *Studies on the growth of the frost layer based on heat and mass transfer through porous media*. Ph.D. thesis, Seoul National University, Seoul.

McConnell, K.G. and Varoto, P.S., 2008. *Vibration Testing: Theory and Practice*. John Wiley & Sons, New Jersey, 2nd edition.

MLA, 2004. "How do I document sources from the web in my works-cited list?" Modern Language Association. 22 Feb. 2007 <http://www.mla.org>.

Rodriguez, O.M.H., Mudde, R.F. and Oliemans, R.V.A., 2006. "Stability analysis of slightly-inclined stratified oil-water flow and intermediate wave theory". In *Proceedings of the 11th Brazilian Congress of Thermal Sciences and Engineering - ENCIT2006*. Curitiba, Brazil.

Shane, C. and Jha, R., 2011. "Proper orthogonal decomposition based algorithm for detecting damage location and severity in composite beams". *Mechanical Systems and Signal Processing*, Vol. 25, pp. 1062–1072.

Trindade, M.A. and Benjeddou, A., 2011a. "Finite element homogenization technique for the characterization of d15 shear piezoelectric macro-fibre composites". *Smart Materials and Structures*, Vol. 20, p. 075012.

Trindade, M.A. and Benjeddou, A., 2011b. "Evaluation of effective material properties of thickness-shear piezoelectric macro-fibre composites". In *Proceedings of the 21st International Congress of Mechanical Engineering - COBEM2011*. Natal, Brazil.

Vanlanduit, S., Parloo, E., Cauberghe, B., Guillaume, P. and Verboven, P., 2005. "A robust singular value decomposition for damage detection under changing operating condtions and structural uncertainties". *Journal of Sound and Vibration*, Vol. 284, pp. 1033–1050.

Wu, C., Liang, Y., Lin, W., Lee, H. and Lim, S., 2003. "Letter to the editor: A note on equivalence of proper orthogonal decomposition methods". *Journal of Sound and Vibration*, Vol. 265, pp. 1103–1110.

10. RESPONSIBILITY NOTICE

The following text, properly adapted to the number of authors, must be included in the last section of the paper: The author(s) is (are) the only responsible for the printed material included in this paper.